Plant, Cell & Environment

WILEY

Plant, Cell & Environment

TECHNICAL REPORT OPEN ACCESS

The Green Index: A Widely Accessible Method to Quantify the Degree of Greenness of Photosynthetic Organisms

Santiago Signorelli[1,2] | Esteban Casaretto[1] | Magdalena Etchemendy-Gamundi[1] | Marcel Bentancor[3] | A. Harvey Millar[2]

[1]Food and Plant Biology Group, Departamento de Biología Vegetal, Facultad de Agronomía, Universidad de la República, Montevideo, Uruguay | [2]ARC Centre of Excellence in Plant Energy Biology, School of Molecular Sciences, The University of Western Australia, Crawley, Western Australia, Australia | [3]Laboratorio de Biología Molecular Vegetal, Instituto de Química Biológica, Facultad de Ciencias, Universidad de la República, Montevideo, Uruguay

Correspondence: Santiago Signorelli (ssignorelli@fagro.edu.uy)

Received: 6 June 2025 | **Revised:** 22 July 2025 | **Accepted:** 23 July 2025

Funding: S.S. is supported by the CPR scheme of the International Centre of Genetic Engineering and Biotechnology (ICGEB), project number ICGEB_URY21_04_EC_2021, the CSIC I + D programme (Uruguay), project number CSIC_I + D_2020_21, and CSIC I + D groups programme (Uruguay), group name: "Food and Plant Biology" and group number '883431'.

Keywords: chlorophyll | leaf | phenotyping | RGB | stress marker

ABSTRACT

Image-based plant phenotyping involves the quantitative determination of complex plant traits using image analysis. One important parameter to assess is the degree of greenness of photosynthetic tissues, as it may reflect plant health, development, or the pigment-depleting impact of stressful environments. Various attempts have been made to quantify leaf greenness scores, but each has shown restricted utility and efficacy. Often, these methods overlooked the precision needed to represent greenness differences. Here, we developed an improved method, the 'Green Index' (GI), to quantitatively score the greenness of photosynthetic tissues and track smooth transitions in seedling greening during de-etiolation. GI is open-source, uses widely available RGB values from image pixels, and does not require advanced computational skills (available at www.foodandplantbiology.com). We describe the conception of the GI formula and evaluate its superiority over existing methods using both literature-derived and new datasets. Furthermore, we demonstrated the utility of the GI in addressing common issues encountered in assessing plant phenotype in biology experiments, underscoring its potential as a reliable and accessible tool. Based on greenness, GI quantitatively discriminates leaf health, developmental stages, and stress sensitivity. We also report that GI significantly correlates with chlorophyll content, and can thus serve as a proxy for tracking chlorophyll trends.

1 | Introduction

Plant phenotyping focuses on the quantitative determination of complex plant traits such as anatomical, physiological and biochemical properties (Fiorani and Schurr 2013). The growing accessibility of imaging technologies and image analysis software has enabled the expansion of non-destructive phenotyping platforms, both in controlled environments and field conditions (Furbank and Tester 2011; Tao et al. 2022; Zavafer et al. 2023). Among the traits commonly assessed, leaf colour is a key indicator of plant health, as it reflects chlorophyll content, nutrient status, and the presence or absence of biotic and abiotic stress (Liang et al. 2017a).

However, colour perception by the human eye is subjective and influenced by lighting and individual interpretation

(Webster 2009). To address this, several systems have been developed to standardize colour quantification. One of the earliest and most influential is the Munsell colours system, which defines colour in terms of hue, value (lightness), and chroma (saturation) (Munsell 1912; Nickerson 1946). Despite the utility of the Munsell system, it is not the colour system that dominates digital images. Instead, digital images quantify colours using RGB (Red, Green, Blue), CMYK (Cyan, Magenta, Yellow, Key or Black), HSL (Hue, Saturation, Lightness), HSV (Hue Saturation Value) and PMS (Pantone Matching System) standards for a variety of technological reasons.

Like Munsell, some of these systems define colours based on variables such as hue, saturation, lightness, value or brightness. A notable exception is RGB, which defines colours by simply adding the three primary colours (Red, Green and Blue). RGB generally represents what is seen by the human eye, as the three types of humans-cone are sensitive mainly to reddish, greenish, and bluish thirds of the visible spectrum (Trussell et al. 2005; Hunt and Pointer 2011). However, it is widely acknowledged that the RGB colour gamut is restricted to the blue-green colours, often leading to professional printers preferring CMYK (McGavin et al. 2005). Despite these limitations in blue-green representation, today, it is RGB that dominates as a standard in digital images for the Internet, most computers, printers, and many low- to medium-end consumer digital cameras and scanners (McGavin et al. 2005). This followed the creation and adoption of the RGB cooperative by HP and Microsoft in 1996 (Stokes et al. 1996) and its standardisation by the International Electrotechnical Commission (IEC) in 1999 (International Electrotechnical Commission 1999).

Several greenness indices have been developed using RGB values, aiming to quantify the proportion or intensity of green in plant images. These include:

$$Green\ Difference = G - \frac{R+B}{2} \tag{1}$$

$$Green\ Difference\quad 2 = \left\{255 + G - \left(\frac{R+B}{2}\right)\right\}/2 \tag{2}$$

$$Vegetation\ Index = 2G - R - B \tag{3}$$

$$Vegetation\ Index\quad 2 = \frac{R-B}{R+B} \tag{4}$$

$$Greenness\ Index = \frac{G}{G+R+B} \tag{5}$$

$$Green\ Leaf\ Index = \frac{2G-R-B}{2G+R+B} \tag{6}$$

$$Greenness = \frac{2G-R-B}{2R+G+B} \tag{7}$$

The Green Difference methods (1 and 2) are often used in photography to identify green pixels. The Green Difference 2 is a variant of the Green Difference method aimed to avoid negative values. The Vegetation Index was developed to focus on green, identify the leaf area on a picture and contrast it against a non-green background (e.g., soil) (Woebbecke et al. 1995). Kawashima (1998) developed Vegetation Index 2 to estimate chlorophyll content. Similarly, the Greenness Index (method 5), also known as Normalized Greenness Intensity (NGI), is another formula developed with the same purpose (Yuan et al. 2017). Other greenness indices measure the green area over a total area in view, which is different to the Greenness Index (method 5). Green Leaf Index (method 6) (Widlowski et al. 2000; Javornik et al. 2023) is a widely used formula with the same aim and has been incorporated into commercial phenotyping platforms such as the multispectral 3D scanner PlantEye F500 (Phenospex, Heerlen, Netherlands). However, Greenness [method 7, (2022)] is slightly different to Green Leaf Index and is used by commercial phenotyping systems (e.g., Phenospex) under the name Green Leaf Index (Lazarević et al. 2022).

While some of these methods have been used to simply score the greenness of a specific area (Widlowski et al. 2000), others have been used to estimate canopy coverage (Starý et al. 2020; Abutaleb et al. 2021), detect stress responses (Valluvan et al. 2023), and to estimate pigments content (Liang et al. 2017a; Li et al. 2021). Despite their utility, in our own image-based phenotyping experiments with arabidopsis (*Arabidopsis thaliana*) seedlings undergoing de-etiolation (Wijerathna-Yapa et al. 2021), we found that existing greenness indices were often unable to discriminate subtle yet visually perceptible differences in leaf colour. This motivated us to develop a new metric, the 'Green Index' (GI), designed to provide enhanced sensitivity to greenness using RGB values. Note that GI was intended as a relative greenness metric rather than a chlorophyll quantification tool.

GI is easy to calculate using the formula provided in this study, does not require advanced image segmentation, specialised software or advanced skills. Alternatively, GI can be calculated using the GI caclulator templates or the GI software available at www.foodandplantbiology.com or www.foodandplantbiology.fagro.edu.uy. In this study, we describe the rationale and development of the GI formula, compare it performance with existing indices, and demonstrate its applicability across a variety of plant biology contexts, including developmental transitions, nutrient status, and stress responses. Additionally, we evaluated its correlation with chlorophyll content and dependence on different photographic cameras.

2 | Materials and Methods

2.1 | Image Acquisition

Pictures of 24-colour cards and plants (Figures 1, 4 and 13) were taken using a Nikon D7000 digital camera mounted on a photographic stand, with artificial lighting kept constant across all images. These images were used to develop the GI formula. The pictures to evaluate the correlation of GI with pigment contents (Figure 12) were taken inside a lightbox using an iPhone 13 Pro. To assess the reproducibility of GI across devices, we also included images taken with an iPhone Xs smartphone (Figures 13).

A

B

Colour		R	G	B	GI	G dif.	G dif. 2	Veg. I	Veg. I 2	Greeness I.	GLI	Greenness
Turquoise		66	169	159	0.33	57	156	113	-0.41	0.43	0.20	0.25
Orange-yellow		196	144	28	0.25	32	144	64	0.75	0.39	0.13	0.11
French blue		4	164	116	0.48	104	180	208	-0.93	0.58	0.46	0.72
Black		17	19	18	0.26	2	128	3	-0.03	0.35	0.04	0.04
Skylue		91	103	155	0.19	-20	118	-40	-0.26	0.30	-0.09	-0.09
Lime		133	170	45	0.51	81	168	162	0.49	0.49	0.31	0.34
Violet		176	52	119	0.11	-96	80	-191	0.19	0.15	-0.48	-0.37
Darkest grey		48	56	58	0.37	3	129	6	-0.09	0.35	0.03	0.03
Dark green		**45**	**86**	**34**	**0.63**	**47**	151	**93**	**0.14**	**0.52**	**0.37**	**0.44**
Purple		56	24	71	0.25	-40	108	-79	-0.12	0.16	-0.45	-0.38
Yellow		200	178	16	0.24	70	163	140	0.85	0.45	0.24	0.24
Dark grey		95	101	101	0.26	3	129	6	-0.03	0.34	0.02	0.02
Blue		47	91	138	0.26	-2	127	-3	-0.49	0.33	-0.01	-0.01
Pink		171	52	61	0.15	-64	96	-128	0.47	0.18	-0.38	-0.28
Red		158	27	21	0.15	-63	96	-125	0.77	0.13	-0.54	-0.34
Grey		142	151	150	0.19	5	130	10	-0.03	0.34	0.02	0.02
Coral		171	120	103	0.18	-17	119	-34	0.25	0.30	-0.07	-0.06
Blue 2		22	61	154	0.19	-27	114	-54	-0.75	0.26	-0.18	-0.21
Green		**51**	**141**	**60**	**0.98**	**86**	170	**171**	**-0.08**	**0.56**	**0.44**	**0.56**
Light grey		178	180	177	0.13	3	129	5	0.00	0.34	0.01	0.01
Brown		86	48	35	0.30	-13	121	-25	0.42	0.28	-0.12	-0.10
Orange		200	99	21	0.18	-12	122	-23	0.81	0.31	-0.05	-0.04
Navy		4	31	120	0.17	-31	112	-62	-0.94	0.20	-0.33	-0.39
Lightest grey		196	199	192	0.10	5	130	10	0.01	0.34	0.01	0.01
					MIN	**0.10**	-96	80	-191	-0.94	0.13	-0.54	-0.39
						0.54	4	130	9	-0.04	0.35	-0.04	0.17
					MAX	**0.98**	104	180	208	0.85	0.58	0.46	0.72

Poor score — Good score

FIGURE 1 | Greenness scores for 24 different colours by multiple methods. (A) 24-Colour card used in this study to analyse the greenness score for each colour using different methods. (B) RGB values for each colour and the scores obtained with the different methods presented in the introduction of this study. Red fills indicate bad scores, whereas green fills indicate good scores. Vegetation Index 2 is known to negative correlate with chlorophyll content; therefore, we inverted the conditional formatting for this formula to allow seamless comparison with other greenness indices.

To test the performance of GI in leaves subjected to different treatments, we analysed leaves or whole plant images from different studies. In particular, to test our GI method, we selected different open access research articles to cover studies having samples with different developmental stages (e.g., de-etiolation and senescence), or subjected to abiotic (e.g., light conditions, salinity, osmotic stress, oxidative stress) and biotic stressors, different nutrient availability, and treatments with phytohormones. Screenshots of the relevant figures displaying slight differences in greenness by eye were taken and open with RawTherapee programme to get the RGB values (explained in 3.2). Figures 2 and 3 reproduce parts of Figure 1 from Wu et al. (2016). Figure 4 reproduces parts of Figure 2 from Wijerathna-Yapa et al. (2021). Figures 5–7 reproduce parts of Figures 1, 2 and 5 in Sakuraba et al. (2014). Figure 8 reproduces parts of Figure 7 from Koyama et al. (2017). Figure 9 reproduces parts of Figure 1 from Kim et al. (2015). Figure 9A,B reproduces a Figure from Hao et al. (2019), while Figure 9C in our manuscript reproduces a part of Figure 4 from Hao et al. (2016). Figure 11 in our manuscript reproduces Figure 3 from Liang et al. (2017a). All the figures reproduced in the present manuscript are free to be reproduced under the Creative Commons Attribution 4.0 International License (http://creativecommons.org/licenses/by/4.0/).

2.2 | Colour Threshold for GI Formula Development

First, we analysed the picture or a 24-colour card using the Colour Thresholder app, within the Image Processing Toolbox MathWorks. Subsequent application to RGB channels defined the range of RGB values, excluding all colours but greens that can be found in leaves (a pale and darker green) (see Video S1 and Figure S1D). Second, we defined the specific values within those ranges that gave the highest score for green. Likewise, we applied the same RGB thresholds to photos of *Arabidopsis* (*A. thaliana*) seedlings on agar plates confirming that those RGB thresholds exclude all the pixels of the picture except the leaves themselves. With this input, we proceeded to the mathematical development of the formula as detailed in the Results section.

2.3 | RGB Determination

During formula development, RGB values were obtained using Affinity Photo and the Colour Picker tool. For the rest of the study, we used the RawTherapee programme as described in the Results section. RGB values vary across different programmes (or even within the same programme) if they are opened using different colour formats and profiles. Therefore, we ensured consistent colour format was used when opening multiple picture files.

An exception was Figure 9C, which displays a GI-based heatmap over leaf images. For this, we did GI calculation and visualisation from image pixels. While not central to the current study, it facilitated the spatial representation of GI values in this particular case.

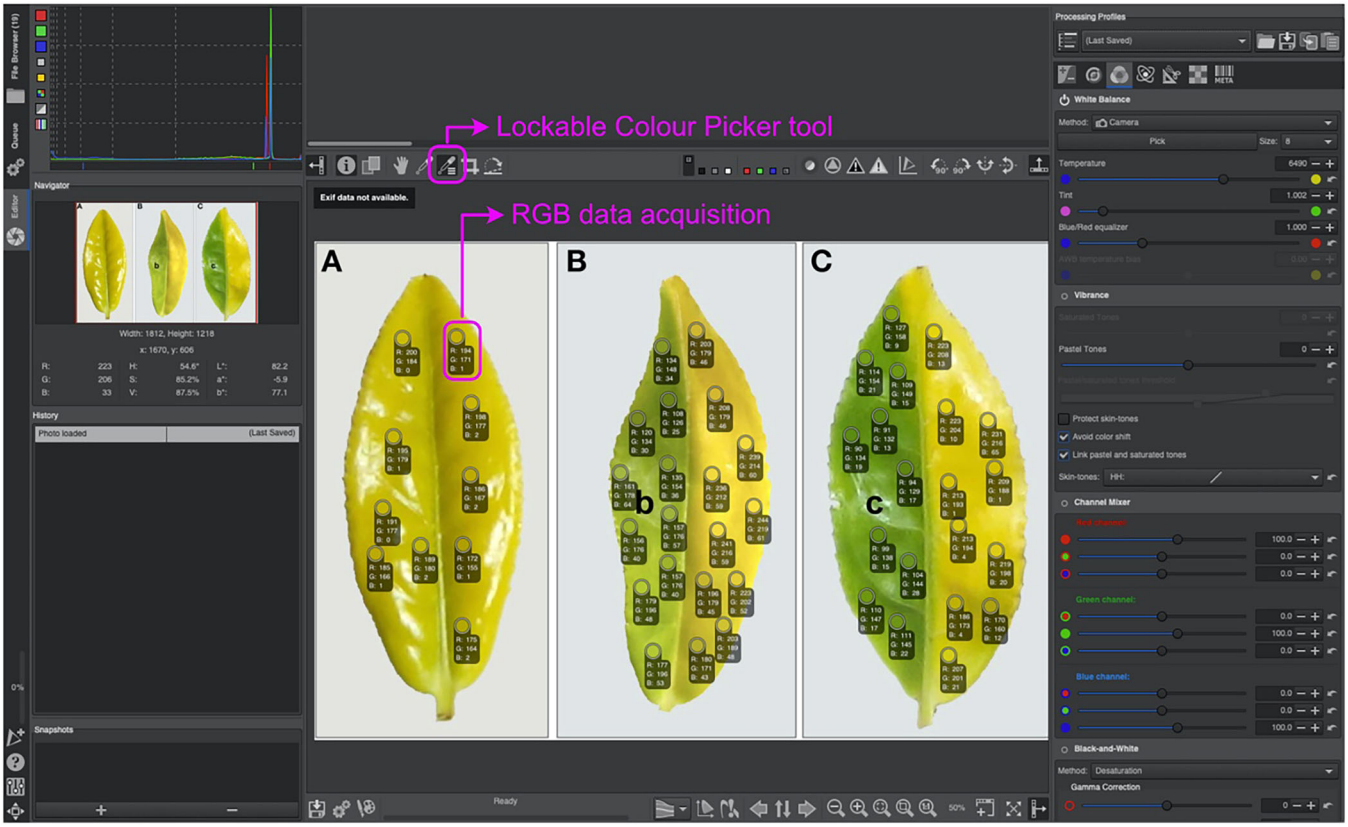

FIGURE 2 | Collecting RGB values form an image using the open-access software RawTherapee. The figure shows the Lockable Colour Picker tool, which can be used to select an area of interest in an image to obtain the RGB values. Multiple examples of the RGB values obtained for different areas of interest are recommended. Here, 10 technical replicates were used per leaf/treatment. [Color figure can be viewed at wileyonlinelibrary.com]

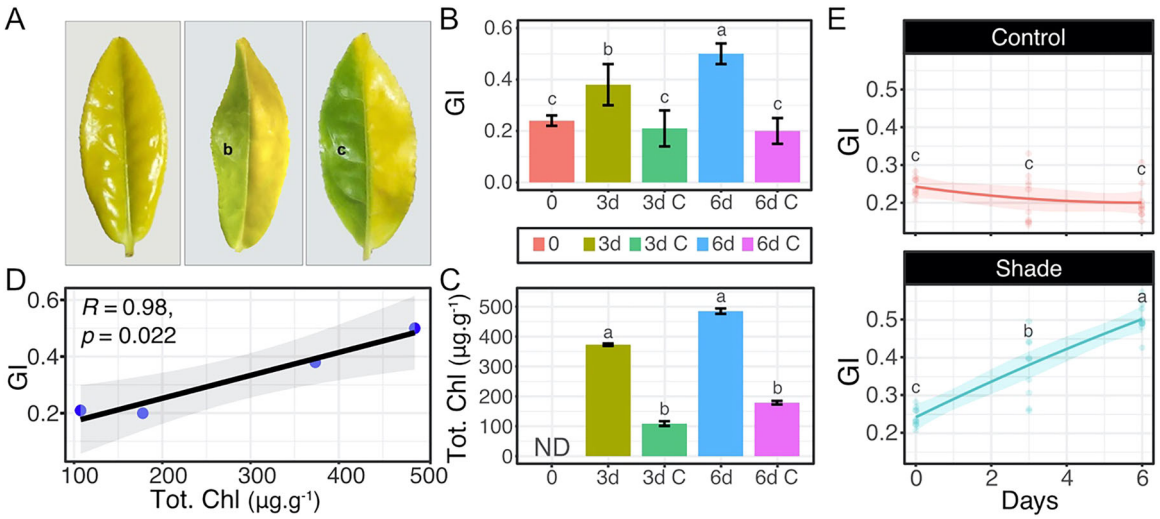

FIGURE 3 | GI of leaves exposed to different light treatments. (A) Leaves exposed to different light treatments: b, 3 days of shade; c, 6 days of shade, as described in Wu et al. (2016). (B) Effect of different treatments on the GI. (C) Total chlorophyll as reported by Wu et al. (2016). (D) Linear regression and Pearson correlation between GI and total chlorophyll content. (E) Effect of different treatments on the GI along the time course studied. Different letters indicate statistical significance differences in an ANOVA Tukey test $p < 0.05$. Panel A was obtained from Wu et al. (2016). [Color figure can be viewed at wileyonlinelibrary.com]

2.4 | Dark-Induced Senescence Experiment

Arabidopsis seeds, accession Col-0, were sown on 3:1:1 peat:-perlite:vermiculite mix and covered with a transparent cover until seedlings were established. Soil was kept moist watering them once a week. Plants were grown in a controlled growth chamber maintaining a photoperiod of 12 h light (21 C): 12 h dark (18 C) with a photon flux of 110 mmol m^{-2} s^{-1} and a relative humidity of 45%–80%. To induce chlorosis and leaf senescence mature leaves of 6- to 8-week-old plants were covered

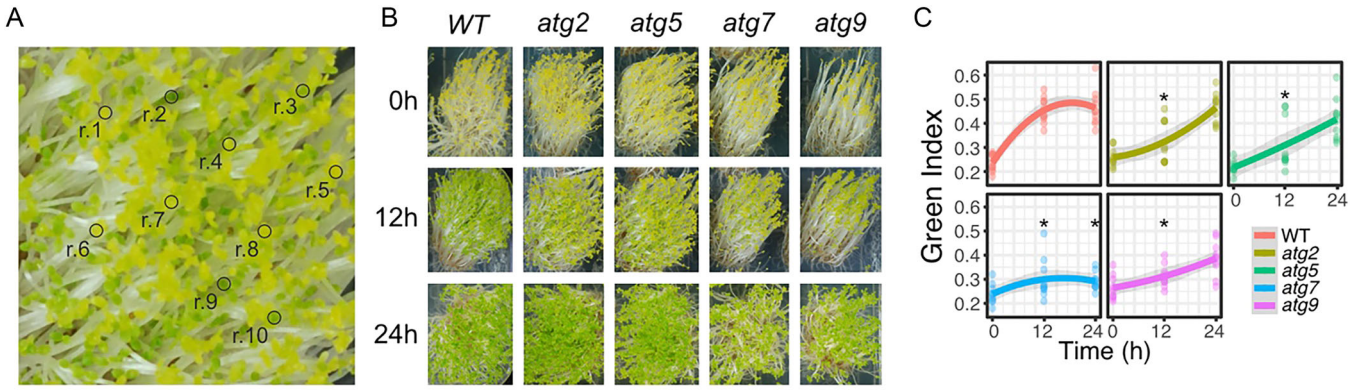

FIGURE 4 | Green Index of etiolated *Arabidopsis* seedlings exposed to light. (A) Magnification of one of the genotypes tested to show the selection of replicates. (B) Visual phenotype of the 5 genotypes after 0, 12 and 24 h of light treatment. (C) Green Index of the 5 genotypes tested at 0, 12 and 24 h after light exposure ($n = 10$). The grey regression represents ±95% confidence level intervals for prediction for the polynomial regression. Asterisks indicate statistically significant differences ($p < 0.05$) by Tukey's HSD test compared to WT at the corresponding time. Data obtained from Wijerathna-Yapa et al. (2021). [Color figure can be viewed at wileyonlinelibrary.com]

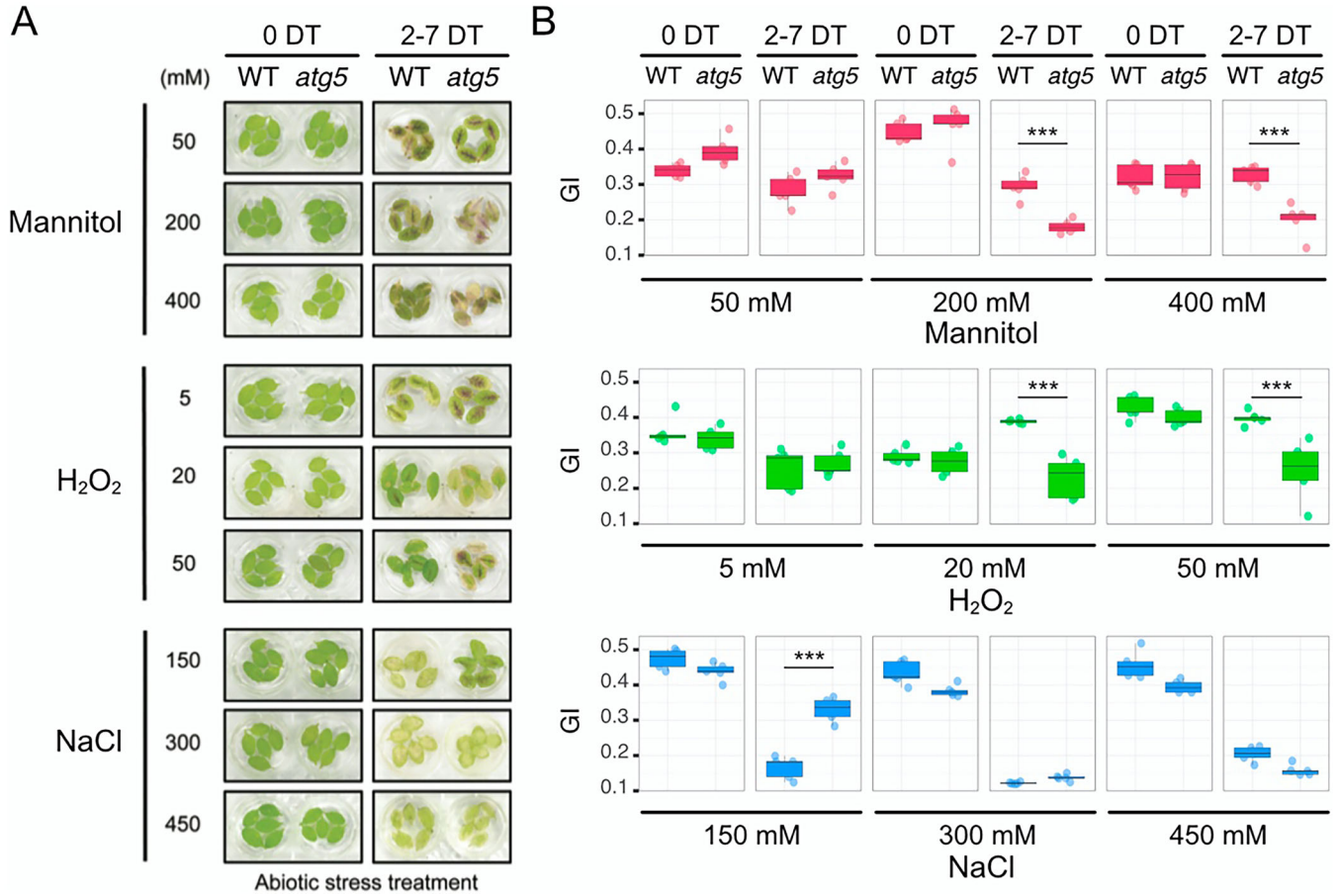

FIGURE 5 | Green Index of *Arabidopsis* leaves exposed to different types of abiotic stress. (A) Phenotype of WT and atg5 leaves exposed to different concentrations of Mannitol, H_2O_2 and NaCl after 0 and 7 days of treatment. (B) Green Index data for the samples shown in (A). Asterisks indicate statistically significant differences (***$p < 0.001$) by Tukey's HSD test compared to WT. Figure in panel A was obtained from Sakuraba et al. (2014). [Color figure can be viewed at wileyonlinelibrary.com]

with aluminium foil for 11, 8, 6, 4, or 1 day. Immediately after removing the aluminium foil, pictures were taken to calculate GI and samples were processed for pigment extraction as described below.

2.5 | Chlorophylls and Carotene Quantification

Individual leaves were transferred to pre-weighted 1.5 mL microtubes and we added 0.8 mL of extraction solution composed

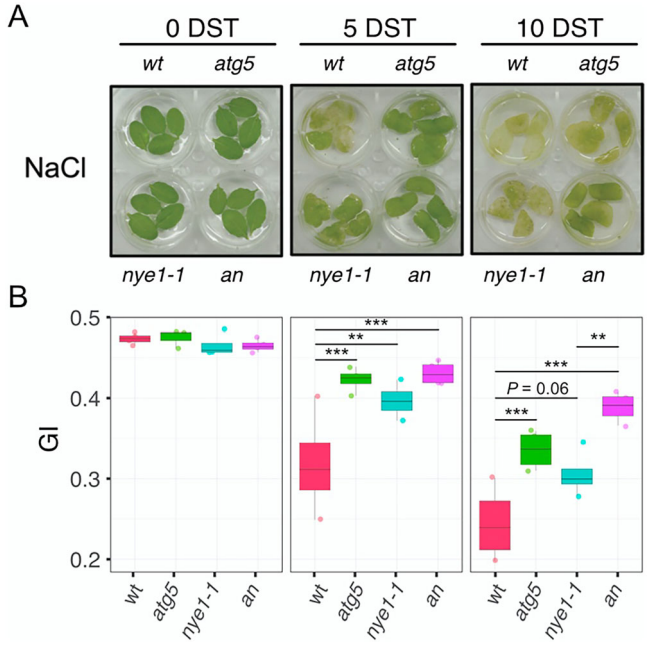

FIGURE 6 | GI of *Arabidopsis* leaves exposed to 150 mM NaCl as a means for inducing abiotic-stress dependent senescence. (A) Phenotype of WT, *atg5*, *nye1-1* and double mutants atg5 nye1-1 (an) leaves exposed to NaCl 150 mM during 5 and 10 days. (B) GI data for the samples shown in (A). Asterisks indicate statistically significant differences (**$p < 0.01$; ***$p < 0.001$) by Tukey's HSD test compared to WT. The figure in panel (A) was obtained from Sakuraba et al. (2014). [Color figure can be viewed at wileyonlinelibrary.com]

of chloroform:methanol (10:1) mixed with a micropestle for 1 min and centrifuged at 5000*g* for 1 min. The liquid phase was taken very slowly to avoid the formation of a turbid solution, and carefully placed in a glass cell for spectrophotometer quantification (Jasco, model V-730, Japan). The extraction solution was used as a blank and the absorbance at 665.5 nm, 647.6 nm and 480 nm were recorded. The concentration of chlorophylls and carotenes were calculated as:

$$\text{Chlorophyll a:}\quad 11.47 \times (Abs.\ 665.5) - 2 \times (Abs.\ 647.6)$$

$$\text{Chlorophyll b:}\quad 21.85 \times (Abs.\ 647.6) - 4.53 \times (Abs.\ 665.5)$$

$$\text{Carotenes:}\quad \frac{(1000 \times Abs.\ 480) - (1.33 \times [Chlorophyll\ a]) - (23.93 \times [Chlorophyll\ b])}{202}$$

as suggested by Lichtenthaler and Wellburn (1983) and Wellburn (1994).

2.6 | Statistical Analysis

Statistical analyses were performed using one-way analysis of variance followed by Tukey's HSD test, with $p < 0.05$ considered statistically significant. Pearson correlation coefficients were calculated using the 'ggpubr' package in R.

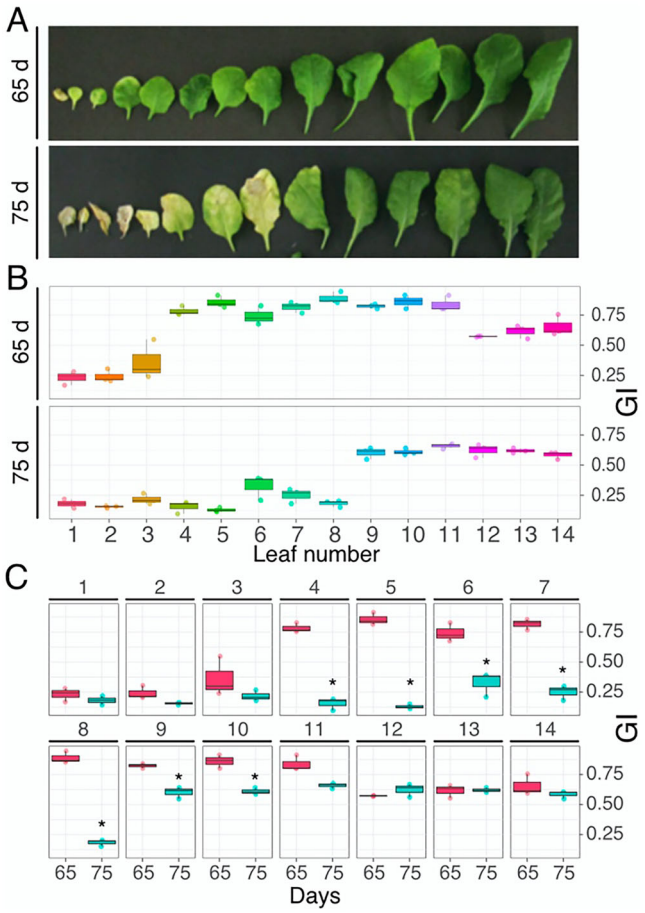

FIGURE 7 | GI of *Arabidopsis* leaves during senescence. (A) Phenotype of 65- and 75-day-old *Arabidopsis* leaves. (B) GI data grouped by age. (C) GI data grouped by leaf number. Asterisks indicate statistically significant differences by Tukey's HSD test. The figure in panel (A) was obtained from Koyama et al. (2017). [Color figure can be viewed at wileyonlinelibrary.com]

2.7 | Figures Elaboration

We used the open source programme R to perform all the plots presented in this study. Plots, plant images and all other components were integrated using Affinity Photo and/or Designer for figure elaboration with a colour format RGB/8 and a colour profile wide Gamut RGB.

3 | Results

3.1 | Green Index Formula Development

RGB values refer to the levels of red (R), green (G) and blue (B) in a coloured pixel and have numerical ranges between 0 and 255. Therefore, any coloured photo can be expressed in RGB. RGB values for each photo pixel can be obtained with many basic image processing programmes because they are the IEC standard for colour in digital images (International Electrotechnical Commission 1999). However, anecdotally, we found that some methods 1–7 did not adequately represent what we observed as different levels of greenness by eye. As an initial approach, we developed a formula, here called $preGI_a$, in which

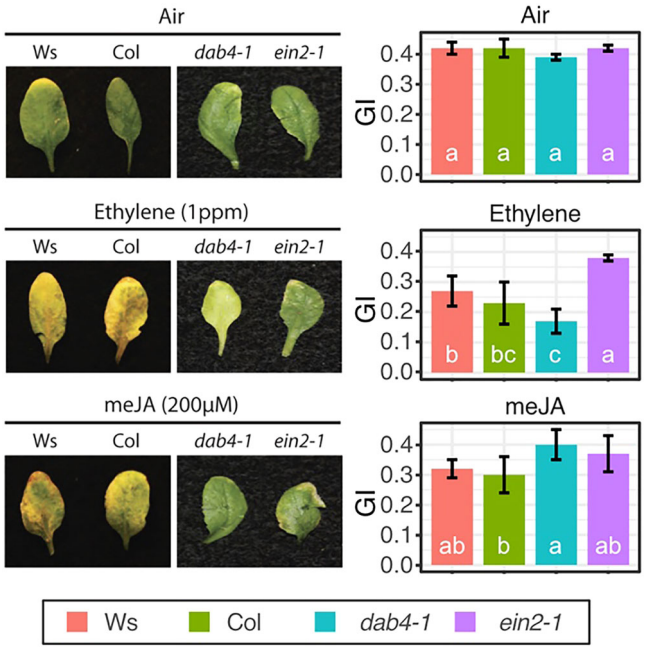

FIGURE 8 | GI of *Arabidopsis* leaves of different genotypes during senescence upon exposure to air, ethylene and meJA. Phenotype of Columbia (Col), Wassilewskija (WS), *dab4-1* (Jasmonic Acid receptor mutant) and *ein2-1* (ethylene insensitive mutant) exposed to air, ethylene and meJA, obtained from Kim et al. (2015), and their respective GI values. Different letters indicate statistically significant differences by Tukey's HSD test. [Color figure can be viewed at wileyonlinelibrary.com]

the R and B components of a pixel decreased its value, whereas the G component value gave a maximum when it was 100, and the values were divided by 255. In this way $preGI_a$ values always sit between 0 and 1, as follows:

$$preGI_a = \frac{(255 - |G - 100|) + (255 - R) + (255\text{-}B)}{3 * 255}$$

A picture of a 24-colour card was used to collect RGB values of each colour hue (Figure S1A) to test this preliminary formula. We observed that the pre-GI_a of a black square was high, and the difference between green and some other colour hues was poor (Figure S1B). To better define which RGB values should score higher, we analysed the 24-colour card with the Colour Thresholder app from MATLAB®. By adjusting the different windows of each colour channel, we noticed that values from 75 to 255 for G and 0 to 75 for R and B allowed us to selectively pick green hues, excluding other colours (Figure S1C–D). The Supplemental Video explains this process. Based on this observation, we concluded that values around 165 (middle point between 75 and 255) should score the most for G and around 37.5 (middle point between 0 and 75) should score the most for R and B. We introduced this consideration in an improved version of the formula as follows:

$$preGI_b = \frac{(255 - |G - 165|) + (255 - |R - 37.5|) + (255 - |B - 37.5|)}{3 * 255}$$

The new formula, $preGI_b$, gave the highest scores to the different green colour hues tested (Dark Green and Green both getting values close to 1 (Figure S1B). To maximise the difference between green hues and any other colour, we divided $preGI_b$ by the difference between 1 and $preGI_b$ to generate $preGI_c$ as follows:

$$preGI_c = \frac{preGI_b}{1 - preGI_b}$$

$preGI_c$ implies that the $preGI_b$ is divided by a small number for green and bigger numbers for a colour different to green, thus maximising the differences between colours as observed in Figure S1B. Due to this addition to the formula, the results are no longer within the range of 0 and 1 and can yield very high values (e.g., when divided by a number near 0). We observed values as high as 11.8 from the 24-colour card. We therefore decided to normalize the data by dividing $preGI_c$ by 12 to get most values between 0 and 1. The final GI was produced as follows:

$$GI = \frac{preGI_c}{12}$$

The results of analysing a 24-colour card suggest that this equation for GI method discriminates very well between different green values and saturations and any other colour hue.

The following equation represents the GI calculation independent of its derivation:

$$\begin{aligned} &Green\ Index\ (GI) \\ &= \frac{\begin{aligned}&[(255 - |G - 165|) + (255 - |R - 37.5|) \\ &+ (255 - |B - 37.5|)]\end{aligned}}{3 * 12 * 255 * (1 - [((255 - |G - 165|) + (255 - |R - 37.5|) \\ &+ (255 - |B - 37.5|))/(3 * 255)])} \end{aligned}$$

In a spreadsheet programme such as Excel®, the formula can be written as:

$$\begin{aligned} GI = ((((&255 - ABS(G - 165)) + (255 - ABS(R - 37.5)) \\ &+ (255 - ABS(B - 37.5)))/(3*255)) \\ &/(1 - (((255 - ABS(G - 165)) + (255 \\ &- ABS(R - 37.5)) + (255 - ABS(B - 37.5))) \\ &/(3 * 255))))/12 \end{aligned}$$

where the ABS function is used to indicate absolute value, and G, R and B should be replaced by the spreadsheet cells containing 0−255 values for each colour. We then systematically compared the results of the GI formula with the results obtained with other methods based on RGB values (methods 1–7). None of the other methods provides good correlations with green value and saturation and, in many cases, colour hues different to green were given a higher score over green (Figure 1). Since these methods were mostly designed to discriminate leaf colours, and not a wider range of colours,

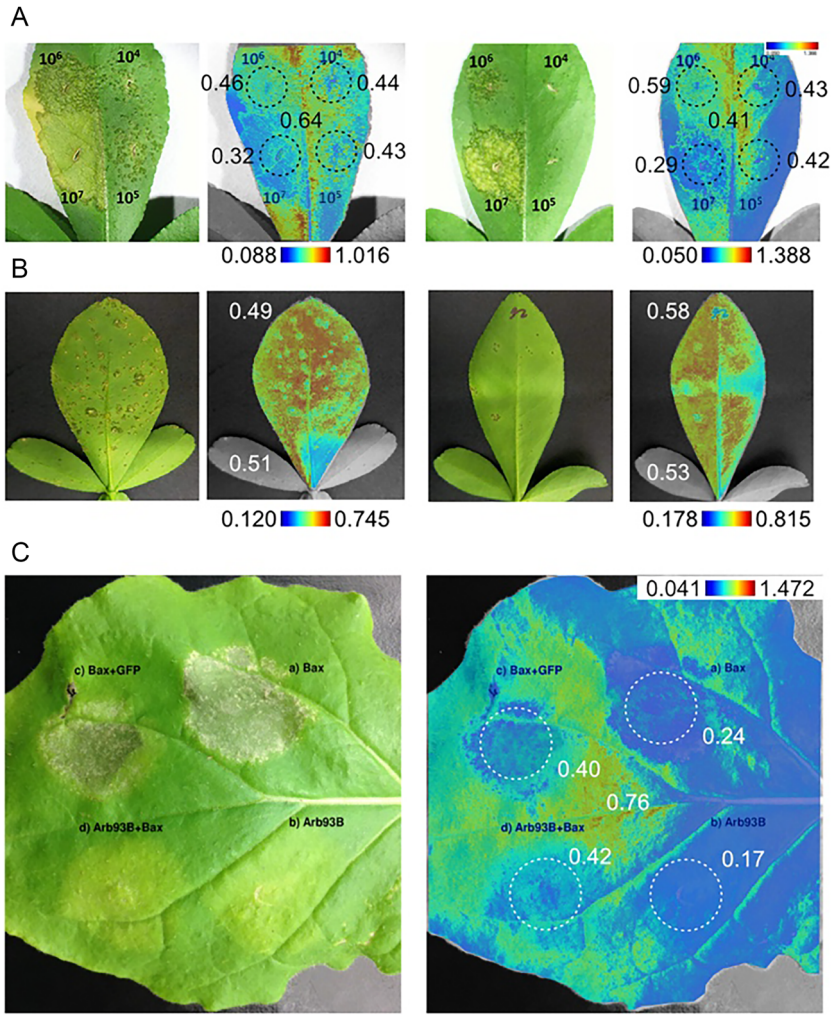

FIGURE 9 | GI surfaces for the study of biotic stress. (A) Image and GI surface for control (left) and transgenic (right) Carrizo citrange leaf infiltrated with 10^4 to 10^7 CFU/mL of *Xanthomonas citri* strain 3213 (modified from Hao et al. 2016). The circlular dashed line indicate the area used to quantify GI, and the value next to each cicrle indicate the GI value. The value in the centre of the figures indicate a reference GI outside the infection zone. (B) Image and GI surface for control (left) and transgenic (right) Carrizo citrange leaf spray-inoculated with 10^6 CFU/mL of *Xanthomonas citri* strain 3213 (modified from Hao et al. 2016). The value at the top indicates the GI of the infected leaf, while the value at the bottom represents the GI for the smaller nonsprayed leaves. (C) Image and GI surface for Bax- (Bcl-2-associated X protein) induced programmed cell death in Tobacco (*Nicotiana benthanmiana*) leaf and its suppression by ARB93B via *Agrobacterium*-mediated transient expression (modified from Hao et al. 2019). The circlular dashed line indicate the area used to quantify GI, and the value next to each circle indicate the GI value. The value in the centre of the figures indicate a reference GI outside the infection zone. [Color figure can be viewed at wileyonlinelibrary.com]

we tested how the performance of the other methods is when scoring greens from leaf images and compare it to GI scoring. Again, GI outperformed the other methods which in most cases fail to discriminate green from yellow hues (Figure S2). Note that GI was not developed based on chlorophyll colour hues, as it is purely intended as a relative greenness metric rather than a chlorophyll quantification tool.

3.2 | Extracting RGB Values From Plant Images

A range of programmes including Photoshop or Affinity Photo allows users to obtain RGB values with one click. However, for this study, we chose to describe the process using the open-source software RawTherapee (rawtherapee.com) available across all computer operating systems. Below we depict the extraction of RGB values for Wu et al. (2016) (Figure 2). We opened the image of interest with RawTherapee, selected the Lockable Colour Picker tool and acquired 10 different areas for each leaf/treatment ($n = 10$). All the R, G and B values were recorded to calculate GI.

We suggest five different biological replicates (e.g., 5 different leaves or plants), with each of them analysed in 4 to 10 different regions for optimal results. However, we recognise this recommendation is only suitable for certain types of images. For instance, when working with developing seedlings, such as those shown in Figure 4, we analysed 10 different cotyledons (biological replicates), each of them determined by a single RGB value representing a 5×5 pixel area (technical replicate). This was necessary because of the size of the cotyledon in the images, the fact that they were usually homogeneous in colour, and the heterogeneity

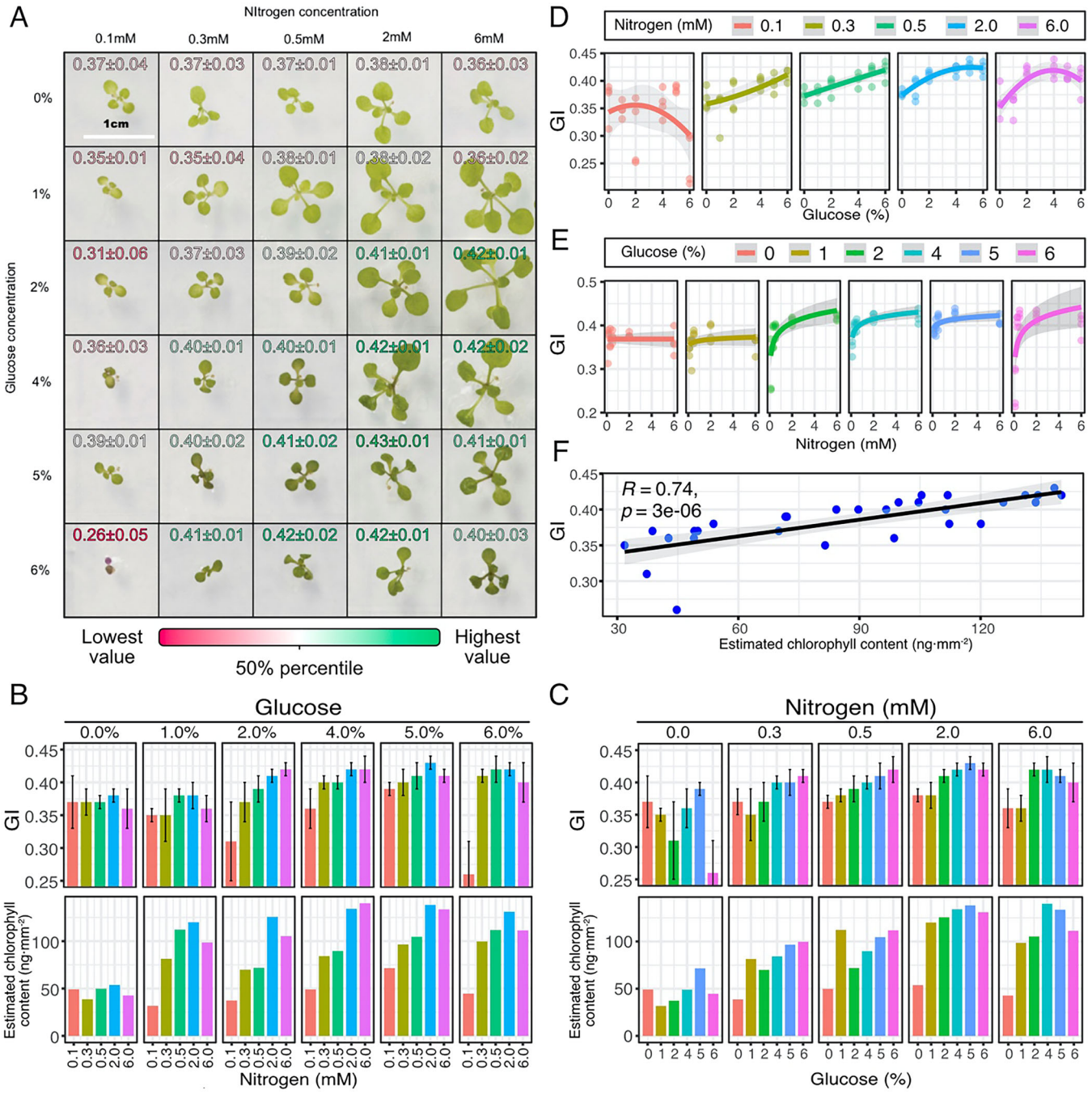

FIGURE 10 | GI analysis of *Arabidopsis* seedlings exposed to different concentrations of glucose and KNO_3. (A) Plant phenotypes and GI values (image taken from Liang et al. (2017)). (B, C) Bar chart of GI values and the estimated chlorophyll content determined by Liang et al. (2017) for different glucose and nitrogen concentrations. T-bars indicate the standard deviation. (D, E) Scatter plots and trend for GI values relative to different glucose and nitrogen concentrations. (F) Correlation between GI values and the estimated chlorophyll content determined by Liang et al. (2017). [Color figure can be viewed at wileyonlinelibrary.com]

between seedlings, which was more relevant than technical replicates.

3.3 | Quantifying GI for Biological Experiments

To best illustrate the value of GI to biologists, we have considered a series of examples of biological processes where greenness changes and estimated GI to quantify experimental images.

3.3.1 | GI Quantification During Different Light Settings

Wu et al. (2016) studied the effect of light on the leaves of *Camellia sinensis* L. cultivar *Baijiguan*, which had an unusual yellow leaf phenotype and, when exposed to low light intensity (or shade), developed a normal green phenotype. Although there is a clear progression in green saturation and value after exposure to shade in their images, the chlorophyll assessment they reported was unable to discriminate between 3 and 6 days

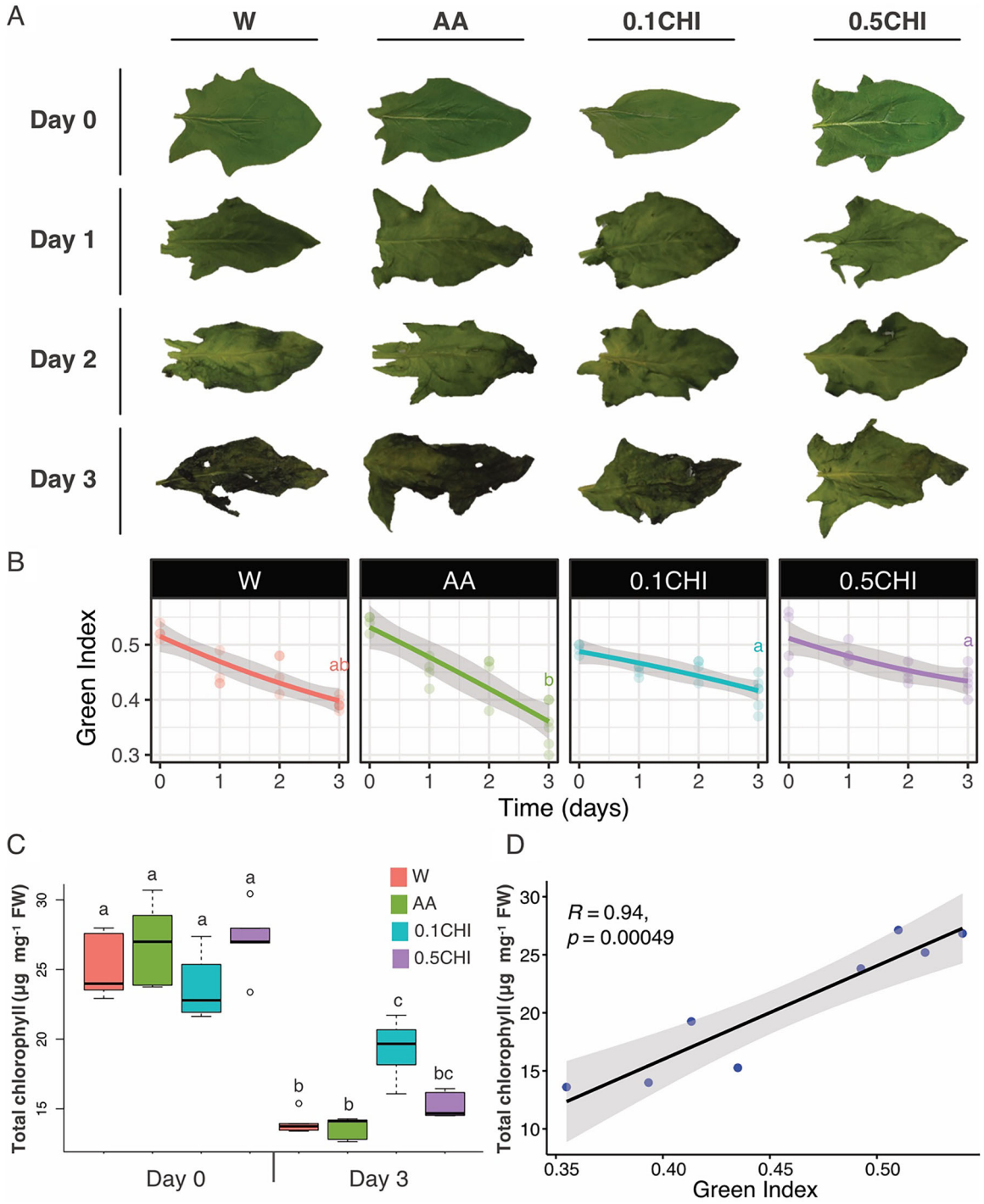

FIGURE 11 | GI analysis of spinach leaves treated with acetic acid and chitosan. Taken from Meitha et al. (2022).(A) Phenotype of leaves. (B) GI. (C) Chlorophyll content. (D) Correlation between chlorophylls and GI. AA, 1% acetic acid (v/v); 0.1CHI, 0.1% chitosan (w/v); 0.5CHI, 0.5% chitosan (w/v); W, water. [Color figure can be viewed at wileyonlinelibrary.com]

of shade treatment (Figure 3A). Nonetheless, GI significantly ($p < 0.05$) discriminated between the shade treatments and their controls on any day and between the different days of shade treatments (Figure 3B). Moreover, GI data mimicked the trends of the total chlorophyll content (Figure 3C). A strong correlation ($R = 0.98$) between total chlorophyll content and GI was also evident by the Pearson correlation coefficient (Figure 3D). Besides the bar plot, we present the data as kinetics (Figure 3E) to show another way of using the GI when a time course experiment is performed.

3.3.2 | GI Quantification in Etiolated Seedlings

In Wijerathna-Yapa et al. (2021), we originally calculated GI to evaluate the greening process in etiolated seedlings of different genotypes. Here, the GI was calculated from different cotyledons. In Figure 4A, we show how heterogeneous the greening of seedlings at 12 h can be, and we illustrate a putative sampling for this phenotype where a combination of green and yellow cotyledons was selected according to their abundance. As observed in Figure 4B, the

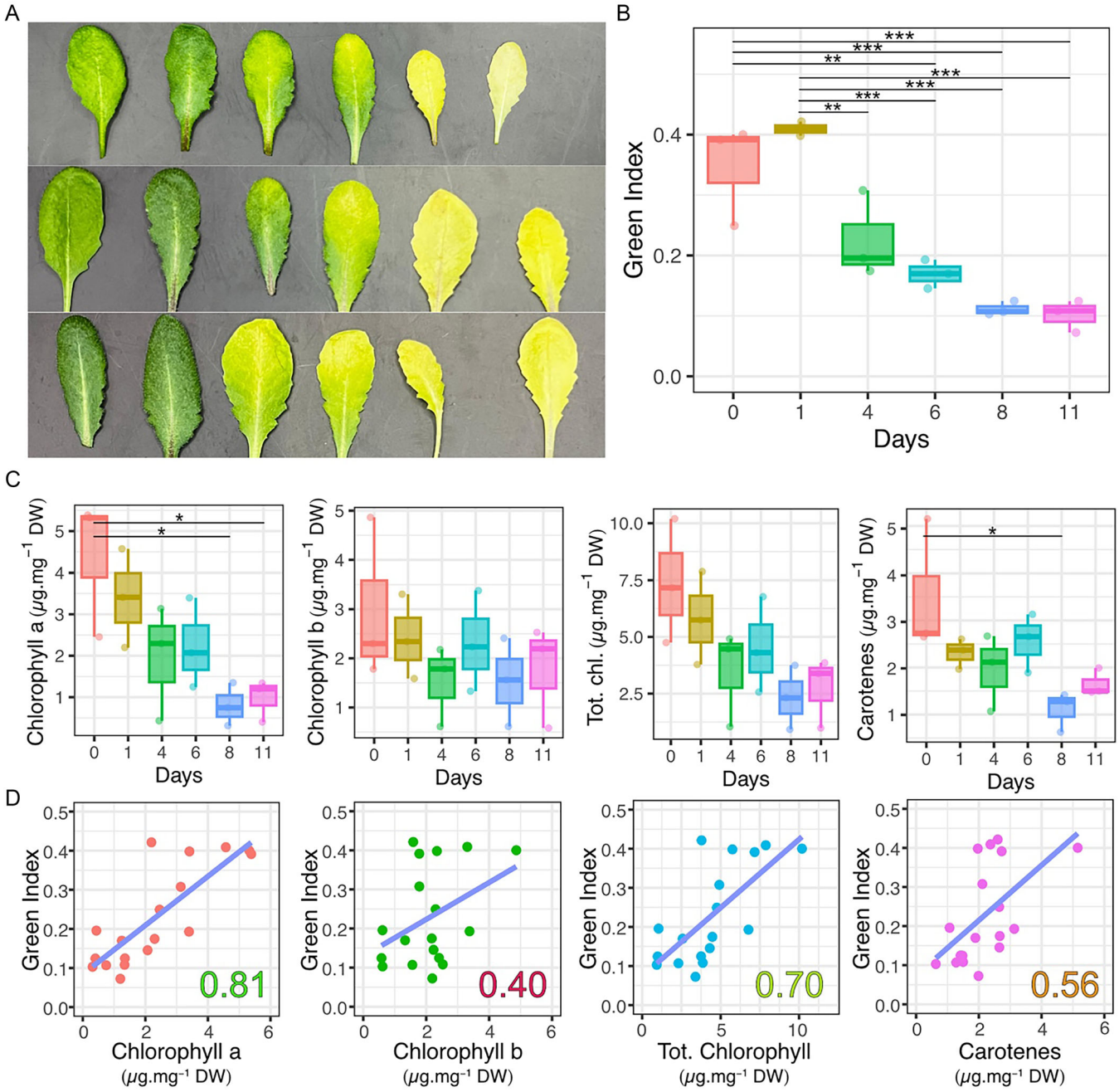

FIGURE 12 | Correlation between GI and the abundance of different pigments. (A) Phenotype of leaves exposed to 0, 1, 4, 6, 8 and 11 (left to right) days of darkness. (B) GI. (C) Pigment abundances on a DW basis. (D) Correlation between pigment abundances and GI. The number in the correlation graphs indicates the Pearson correlation factor and the colour indicates a good (green) or weak (red) correlation. Asterisks show statistical differences based on one-way analysis of variance with Tukey's post hoc honest significant difference testing at $*p < 0.05$, $**p < 0.01$, $***p < 0.01$, $n = 3$. [Color figure can be viewed at wileyonlinelibrary.com]

greenness was more homogenous at 0 h (mostly yellow) and 24 h (mostly green) than at 12 h, and this was clearly reflected in the GI (Figure 4C). Even though there was heterogenicity observed in greenness at 12 h, the Green Index showed statistically significant differences between all the autophagy genotypes and the WT plants at 12 h, but only for one genotype at 24 h, suggesting that most of the genotypes could reach a wild-type state by 24 h (Figure 4C). Thus, the Green Index method was useful for establishing evidence of a statistically significant delay in greening in the autophagy genotypes tested.

3.3.3 | GI Quantification Under Abiotic Stressors

Sakuraba et al. (2014) tested the effect of mannitol, H_2O_2, and NaCl on WT and the autophagy mutant *atg5* (Figure 5A). These compounds are commonly used to impose osmotic, oxidative and saline stress, respectively. The authors took pictures at 0 and 7 days after treatments. GI analyses of their images revealed that 200 mM mannitol was already enough to induce a significant difference between atg5 and WT at 7 days after treatment, whereas no significant differences were observed with 50 mM mannitol (Figure 5B). Likewise, 20 and 50 mM H_2O_2 showed

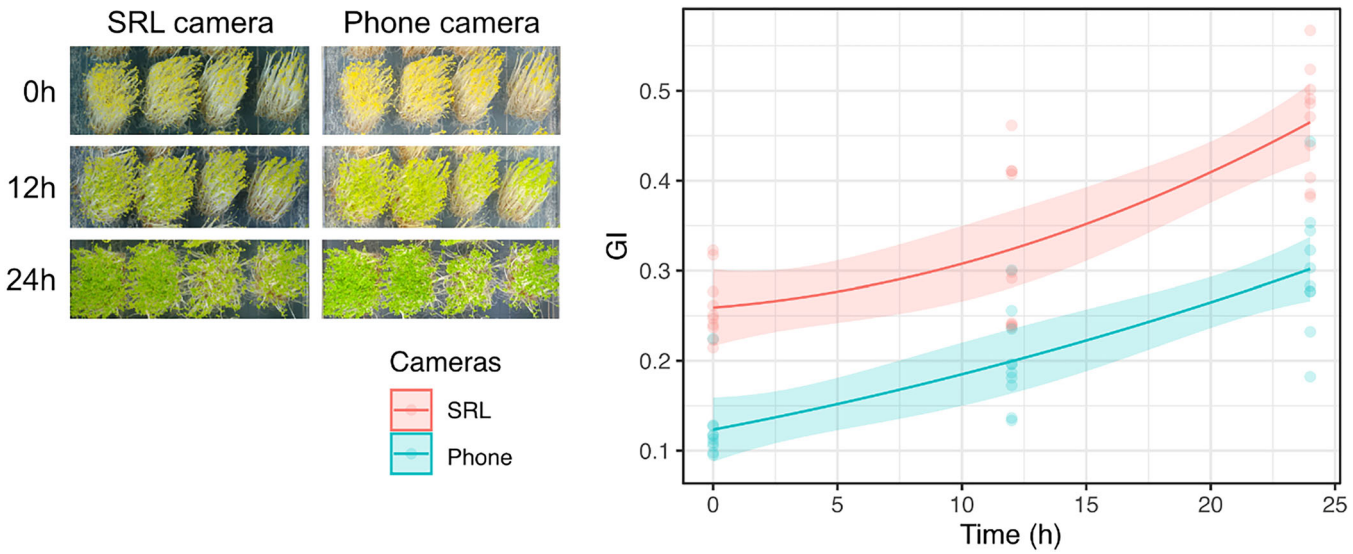

FIGURE 13 | Comparison of GI calculated from pictures taken by a single-lens reflex (SLR) mirrorless camera and a mirror-based phone camera. The image shows de-etiolated arabidopsis *sugar dependent mutant* (*sdp1*) seedlings exposed to light for 0, 12 and 24 h. The graph represents the GI at 0, 12 and 24 h calculated from the SRL and phone camera images. [Color figure can be viewed at wileyonlinelibrary.com]

significant GI differences between these lines, while 5 mM did not. Finally, the lowest concentration of NaCl tested also produced significant differences to the Control in terms of Green Index but not the greatest concentrations (300 and 450 mM), which is consistent with the visuals.

These results show that GI can quantify responses under abiotic stress conditions, and its value correlated very well with the chlorophyll data provided in the same study ($R = 0.82$, $p = 3.3e-5$, Figure S3A).

As observed in Figure 5B, the greater concentrations of NaCl resulted in severe stress for both genotypes and no significant differences were observed. The authors selected the lowest concentrations of NaCl (defined as mild stress) to investigate further the differences at earlier time points in the autophagy mutant (*atg5*) and the nonfunctional stay-green *nonyellowing1-1* (*nye1-1*). We decided to analyse these time points to see if the GI was able to differentiate smaller differences in phenotype. Both 3 and 5 days after treatment, GI values for WT were significantly different to those for *atg5*, while only 5 days after treatment, WT was significantly different to *nye1-1* (Figure S4). Moreover, a strong correlation between GI and chlorophyll content was found ($R = 0.86$, $p = 0.0027$, Figure S3B). This result suggests that GI could identify subtle differences in green saturation and the value of a phenotype when exposed to mild stress.

3.3.4 | GI Assessment in Abiotic Stress-Induced and Naturally Occurring Senescence

We also investigated if GI could be used to assess the degree of senescence in different genotypes or leaves within the same plant. First, we investigated the GI in abiotic stress-induced senescence of WT, *atg5*, *nye1-1*, and the *atg5 nye1-1* double mutant (*an*) (Figure 6). GI showed significant differences between the WT and all lines at 5 days and all but *nye1-1* at 10 days after treatment. Again, a good correlation between GI and chlorophyll content was found ($R = 0.86$, $p = 0.00038$, Figure S3C).

We also investigated the GI in different leaves of senescing plants at two-time points of natural senescing from the data of Koyama et al. (2017) (Figure 7A). GI was able to discriminate well between leaves of the same plant at the same time point (Figure 7B), and in many cases, the values were significantly different when comparing 65 with 75-days-leaves (Figure 7C). Note that the study cited here was not aimed at measuring greenness. Thus, the correct positioning of the leaves and control of light conditions could enhance the differences observed by GI.

3.3.5 | GI Assessment in Phytohormones-Induced Senescence

To further explore the potential of GI in studies of senescence, we compared the GI scores of leaves of the same age for different genotypes and treatments. Kim et al. (2015) analysed the phenotype of senescing leaves of *Arabidopsis* Columbia (Col) and Wassilewskija (WS) ecotypes, together with *dab4-1* (a jasmonic acid receptor mutant) and *ein2-1* (an ethylene insensitive mutant) upon exposure to air, methyl jasmonate (meJA) and ethylene. Under air conditions, the GI were not statistically different, however, under ethylene and meJA, significant differences were observed among the genotypes (Figure 8).

3.3.6 | Using GI to Assess Biotic Stress

We also found that GI could be useful to identify diseased or infected areas of a leaf. Therefore, generated GI surface map and coloured heatmap from RGB images. Using this we determined the GI surface of leaves infiltrated with different concentrations of *Xanthomonas citri* strain 3213 (Figure 9A,B; Hao

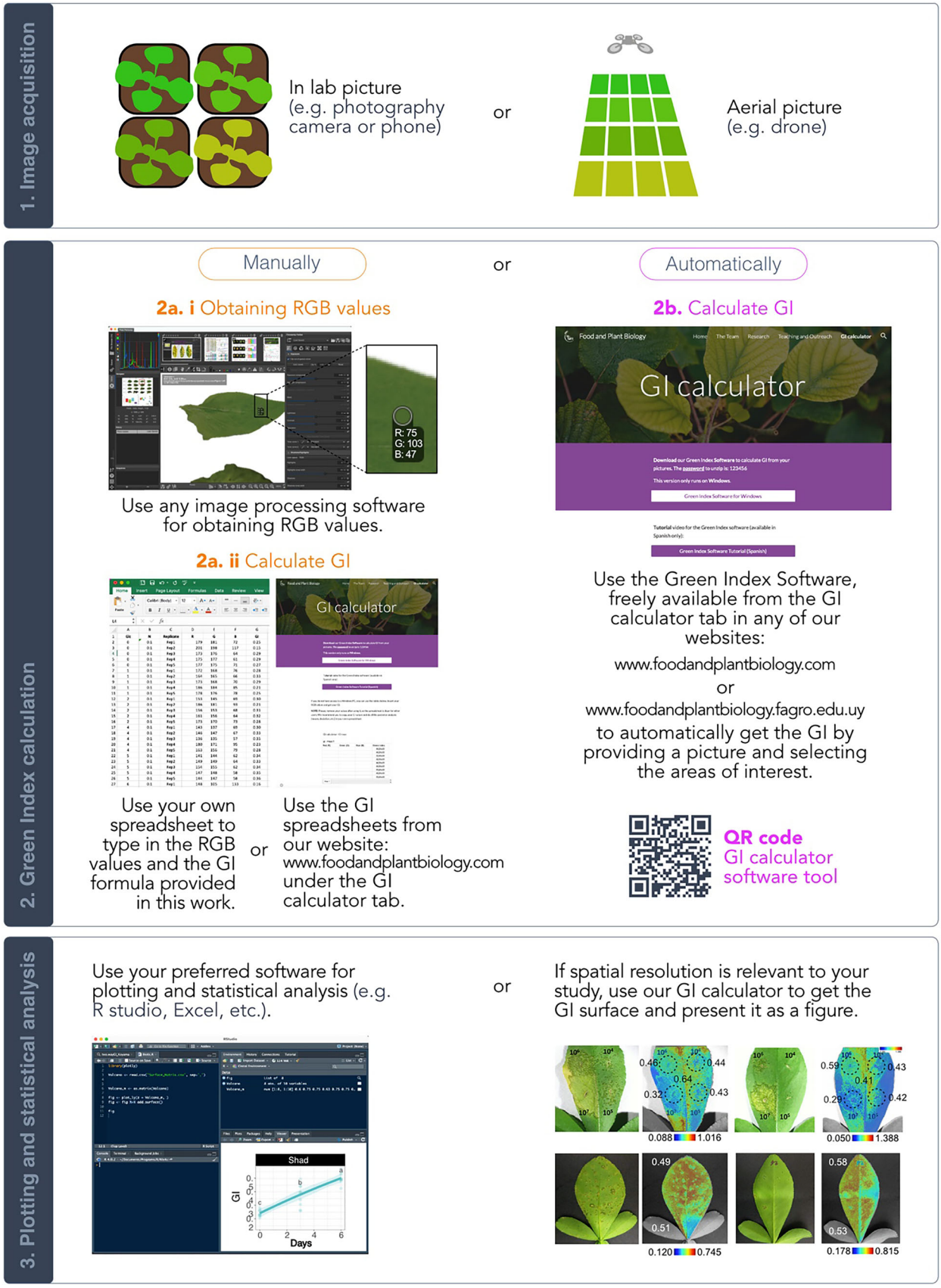

FIGURE 14 | Legend on next page.

et al. 2016) and or with Bax (Bcl-2-associated X protein), which induces programmed cell death (PCD) (Figure 9C; Hao et al. 2019), as well as the co-infiltration of Bax with ARB93B which is suggested to suppress PCD. For the infiltrated leaves (Figure 9A) the lowest GI values were found when the higher concentration of bacteria was applied. In the spray inoculated leaves (Figure 9B) the infection zone was also much more clearly visible in the GI picture, as denoted by bluish-greenish colour, than in the regular picture.

Likewise, in the Bax-infiltrated leaf, the zones of infiltration were clearly marked by low GI values (Figure 9C). However, in Figure 9C there was also a clear effect of the illumination, affecting GI values, in which one half of the leaf is more illuminated than the other due to the curvature of the leaf. These changes in illumination can hinder real differences in terms of greenness and thus it is very important that the picture is taken from a top view in which the leaf is as flat as possible or illuminated from multiple angles.

3.3.7 | GI to Evaluate Nutritional Stress in Seedlings

Liang et al. (2017) phenotyped *Arabidopsis* plants in response to different concentrations of glucose and nitrogen. Using their images, we determined if GI was sensitive enough to quantify the mild differences in green saturation and value of leaves across nutrient treatments. Indeed, the well-nourished leaves score GI values up to 0.43, whereas the most nutrient-depleted plants showed values as low as 0.26 (Figure 10A). The GI results also agreed with the estimated chlorophyll content determined in the original publication for the different concentrations of both glucose and nitrogen (Figure 10B,C). For most concentrations of nitrogen, increasing glucose content showed a positive effect on greenness and thus, GI values. However, the high glucose contents were detrimental to greenness at 0.1 mM KNO_3 (Figure 10D). Nitrogen increased the greenness and GI values, and such an increase grew with increasing concentrations of glucose (Figure 10D). Additionally, we reaffirmed the GI values were significantly correlated with chlorophyll content in this study (Figure 10G).

3.3.8 | GI to Evaluate Chemical Treatment for Postharvest Preservation

Meitha et al. (2022) tested the effect of chitosan on the postharvest preservation of spinach leaves and determined chlorophyll content as one of the parameters to indicate leaf health (Figure 11). GI data was able to discriminate between the days of postharvest and the treatments (Figure 11B). The GI values showed a significant correlation ($R = 0.94$, $p = 0.00049$) with chlorophyll content (Figure 11D).

3.4 | Correlation of Green Index With Different Type of Pigments

The analysis of correlation between GI determined here and the total chlorophylls reported in other studies showed a strong positive correlation (Figures 3, 10, 11, and S3). To further understand the correlation between GI and the amount of different pigments (chlorophyll *a*, chlorophyll *b*, and carotenes) we subjected arabidopsis leaves to darkness for 0, 1, 4, 6, 8 and 11 days to induce leaf senescence and obtain leaves with a range of different greenness (Figure 12A). From day 4 onwards, the GI scores were significantly different to those obtained at 0 or 1 day of darkness, with decreasing values over time (Figure 12A).

Chlorophyll *a*, chlorophyll *b*, total chlorophylls and carotenes all displayed a relationship with GI values (Figure 12C). Unlike GI, the statistical significance for individual pigment data across days of darkness was much more reduced. We attribute this difference to the greater technical error for the methodology to quantify pigments, relative to the GI methodology. When we analysed the Pearson correlation coefficient between GI and the different pigments evaluated, we observed that GI has a strong positive correlation with all pigments evaluated, however, this correlation is strongest with chlorophyll a, then with total chlorophylls, then with carotenes, and a weaker correlation is found between GI and chlorophyll b. These results together with the results from Figures 3, 10, 11 and S3, highlight one of the main advantages of GI: it offers more consistent and statistically powerful discrimination between samples than traditional pigment quantification, while requiring minimal equipment and non-destructive sampling. It is noteworthy however, that it is not possible to provide a specific correlation value or calibration curve between GI and pigments because this will vary depending on the light conditions in which the pictures are taken as well as the device taking the pictures.

3.5 | Comparison of GI Values Obtained With an SLR Versus Smartphone

Given that different cameras have different sensors for different light wavelengths, they can produce different RGB values for the same object and light condition. Moreover, the algorithms for processing the raw data captured by the sensor that is used to produce the image (i.e., the RGB values), as well as the settings (e.g., exposure time, aperture size, ISO sensitivity, etc.), vary across cameras, resulting in different RGB values. To test

FIGURE 14 | Workflow for calculating the Green Index (GI) from plant images. 1. Image acquisition: Pictures can be taken in controlled conditions (e.g., with a camera or phone in the lab) or in the field (e.g., with drones). 2. Green Index calculation: 2a. Manual workflow: RGB values can be extracted using any image processing software (e.g., RawTherapee or Affinity Photo), and GI can be calculated using the formula provided in this study, either in a custom spreadsheet or using pre-configured templates available at www.foodandplantbiology.com and www.foodandplantbiology.fagro.edu.uy. 2b. Automated workflow: The Green Index Software, freely available at the previously mentioned websites, enables automatic GI calculation by uploading an image and selecting areas of interest. A QR code linking to this tool is also presented. 3. Plotting and statistical analysis: GI values can be visualized and analysed using statistical software (e.g., R, Excel). If spatial resolution is important, the software can also generate GI surface maps for detailed visualisation. [Color figure can be viewed at wileyonlinelibrary.com]

the effect of these differences on GI, we compared values from a professional single-lens reflex mirrorless camera (Nikon D7000 digital SLR camera) and a mirror-based phone camera (iPhone Xs). The visuals obtained were different where the phone camera produced more colour–saturated images (Figure 13). This was also reflected by the GI values. Nonetheless, the trend and difference between time points remained constant (Figure 13). So, while the GI of images obtained from different styles of cameras are not constant and cannot be directly compared, any camera is likely to be useful in determining GI as long as the same camera is used during the whole experiment.

4 | Discussion

The GI is an open-source and user-friendly method that treats colour as a quantitative trait. Unlike existing RGB-based indices, GI was mathematically optimised to match visual perception of greenness and to maximise discrimination between biologically relevant colour variations. It enables the objective quantification of photosynthetic greenness, which is often associated with plant health, stress status, and developmental stage. In this study, we demonstrated that GI can effectively distinguish between healthy and stressed leaves, different genotypes, and stages of development. Its simplicity and versatility make it suitable for a broad range of phenotyping applications, from early seedling development to postharvest monitoring.

A key strength of GI lies in its accessibility for researchers in many contexts, with or without laboratory facilities or significant budgets. It can be calculated from standard digital images using widely available software such as RawTherapee or Excel. To further support its accessibility and uptake we have also developed a dedicated software tool to automate the GI calculation from digital images. The current study provides the principles of the methodology that underlies this tool and it is now freely available at www.foodandplantbiology.com, or www.foodandplantbiology.fagro.edu.uy, under the GI calculator tab. In Figure 14 we summarize our current workflow for calculating GI from plant images.

The data presented here highlight the superior performance of GI compared to existing RGB-based indices, particularly in its ability to resolve subtle differences in greenness across biological contexts. GI scores were consistently correlated with chlorophyll content, suggesting that GI can be used as a reliable proxy for chlorophyll trends. This is particularly relevant in situations where tissue quantity is limited or destructive sampling is not feasible. Because GI is calculated from image pixels, it is a noninvasive and scalable method. It holds potential for high-throughput phenotyping, including canopy-level applications using drones or fixed imaging stations. With over 16 billion mobile phones operating in the world in 2023, being 6.9 billion smartphones (Statista 2023), the ability to assess greenness with minimal technical resources is especially valuable for low-resource settings.

One limitation of GI is its sensitivity to lighting conditions, which affects RGB values. To minimise this effect, we recommend standardising light exposure across images and including a colour reference card when imaging on different days or in different environments. Presenting GI as relative values and normalising against a green reference can help reduce variability due to ambient light.

Beyond its simplicity and accessibility, the GI could serve as a foundation for more advanced and scalable applications. Integrating GI-based analysis with machine learning algorithms offers exciting prospects for real-time monitoring of plant health across both controlled and field environments (Singh et al. 2016; Tsaftaris et al. 2016). Such integration could enhance phenotypic predictions by enabling automated pattern recognition and adaptive learning under different growth conditions. Furthermore, recent literature has shown how low-cost phenotyping devices can be developed using 3D printers, smartphones, and off-the-shelf components (Minervini et al. 2016; Gaggion et al. 2021). Incorporating GI into these DIY platforms, with or without AI, could substantially improve their capabilities while maintaining affordability and user-friendliness. Exploring these directions could enhance the global applicability of GI, particularly in resource-limited settings.

5 | Conclusions

We propose the GI as a simple and effective parameter to quantify leaf greenness from digital images. GI is calculated from RGB values, which can be easily obtained using standard software, without the need for advanced computational skills. We demonstrated that GI reliably distinguishes between healthy and stressed leaves, different developmental stages, and responses to biotic and abiotic stress.

Moreover, GI correlates well with leaf chlorophyll content, providing an easy and low-cost alternative to track chlorophyll trends. Its accessibility makes it suitable for a wide range of research contexts, including small-scale lab experiments (e.g., 7-day-old arabidopsis seedlings) and large-scale phenotyping in the field (e.g., canopy-level imaging).

Author Contributions

S.S. conceived the study, developed the GI formula, performed the experiments, analysed the data, prepared the figures, wrote the manuscript, and secured funding. E.C. and M.E.G. quantified chlorophyll content, extracted RGB values from external images, and calculated GI. M.B. developed the software tool for automatic GI calculation. A.H.M. contributed to experimental design, data interpretation, manuscript writing, and funding acquisition.

Acknowledgements

S.S. is a grateful active member of the Uruguayan System of Researchers (SNI, Uruguay) and the Basic Research Development Programme (PEDECIBA, Uruguay). We thank Dr. Mohammad Mukarram for his general comments about our manuscript and helping us to present the different methods as equations. S.S. is supported by the CPR scheme of the International Centre of Genetic Engineering and Biotechnology (ICGEB), project number ICGEB_URY21_04_EC_2021, the CSIC I + D programme (Uruguay), project number CSIC_I + D_2020_21, and CSIC I + D groups programme (Uruguay), group name: "Food and Plant Biology" and group number '883431'.

Data Availability Statement

The data that support the findings of this study are available from the corresponding author upon reasonable request.

References

Abutaleb, K., M. Freddy Mudede, N. Nkongolo, and S. W. Newete. 2021. "Estimating Urban Greenness Index Using Remote Sensing Data: A Case Study of an Affluent vs Poor Suburbs in the City of Johannesburg." *Egyptian Journal of Remote Sensing and Space Science* 24: 343–351.

Fiorani, F., and U. Schurr. 2013. "Future Scenarios for Plant Phenotyping." *Annual Review of Plant Biology* 64: 267–291. https://doi.org/10.1146/annurev-arplant-050312-120137.

Furbank, R. T., and M. Tester. 2011. "Phenomics—Technologies to Relieve the Phenotyping Bottleneck." *Trends in Plant Science* 16: 635–644.

Gaggion, N., F. Ariel, and V. Daric, et al. 2021. "ChronoRoot: High-Throughput Phenotyping by Deep Segmentation Networks Reveals Novel Temporal Parameters of Plant Root System Architecture." *GigaScience* 10: giab052.

Hao, G., S. McCormick, M. M. Vaughan, et al. 2019. "*Fusarium graminearum* arabinanase (Arb93B) Enhances Wheat Head Blight Susceptibility by Suppressing Plant Immunity." *Molecular Plant-Microbe Interactions®* 32: 888–898.

Hao, G., E. Stover, and G. Gupta. 2016. "Overexpression of a Modified Plant Thionin Enhances Disease Resistance to Citrus Canker and Huanglongbing (HLB)." *Frontiers in Plant Science* 22, no. 1: 1078.

Hunt, R. W. G., and M. R. Pointer. 2011. *Measuring color*. John Wiley & Sons.

International Electrotechnical Commission. 1999. *Colour management –Default RGB colour space – sRGB*.

Javornik, T., K. Carović-Stanko, J. Gunjača, M. Vidak, and B. Lazarević. 2023. "Monitoring Drought Stress in Common Bean Using Chlorophyll Fluorescence and Multispectral Imaging." *Plants* 12: 1386.

Kawashima, S. 1998. "An Algorithm for Estimating Chlorophyll Content In Leaves Using a Video Camera." *Annals of Botany* 81: 49–54.

Kim, J., C. Chang, and M. L. Tucker. 2015. "To Grow Old: Regulatory Role of Ethylene and Jasmonic Acid in Senescence." *Frontiers in Plant Science* 6: 1–7.

Koyama, T., F. Sato, and M. Ohme-Takagi. 2017. "Roles of miR319 and TCP Transcription Factors in Leaf Development." *Plant Physiology* 175: 874–885.

Lazarević, B., M. Kontek, K. Carović-Stanko, et al. 2022. "Multispectral Image Analysis Detects Differences in Drought Responses in Novel Seeded *Miscanthus Sinensis* Hybrids." *GCB Bioenergy* 14: 1219–1234.

Li, M., V. Coneva, K. R. Robbins, D. Clark, D. Chitwood, and M. Frank. 2021. "Quantitative Dissection of Color Patterning in the Foliar Ornamental Coleus." *Plant Physiology* 187: 1310–1324.

Liang, Y., D. Urano, K. L. Liao, T. L. Hedrick, Y. Gao, and A. M. Jones. 2017. "A Nondestructive Method to Estimate the Chlorophyll Content of *Arabidopsis* Seedlings." *Plant Methods* 13: 1–10.

Lichtenthaler, H. K., and A. R. Wellburn. 1983. *Determinations of Total Carotenoids and Chlorophylls a and b of Leaf Extracts in Different Solvents*. Portland Press Ltd. in press.

McGavin, D., B. Stukenborg, and M. Witkowski. 2005. "Color Figures in BJ: RGB Versus CMYK." *Biophysical Journal* 88: 761–762.

Meitha, K., Y. Pramesti, S. Signorelli, and J. A. Kriswantoro. 2022. "Postharvest Chitosan Application Maintains the Quality of Spinach Through Suppression of Bacterial Growth and Elicitation." *Horticulture, Environment, and Biotechnology* 63, no. 2 63: 217–227.

Minervini, M., A. Fischbach, H. Scharr, and S. A. Tsaftaris. 2016. "Finely-Grained Annotated Datasets for Image-Based Plant Phenotyping." *Pattern Recognition Letters* 81: 80–89.

Munsell, A. H. 1912. "A Pigment Color System and Notation." *American Journal of Psychology* 23, no. 2: 236–244. https://doi.org/10.2307/1412843.

Nickerson, D. 1946. *Color Measurement and Its Application to the Grading of Agricultural Products*. Munsell Color System, Company, and Foundation.

Sakuraba, Y., S. H. Lee, Y. S. Kim, O. K. Park, S. Hörtensteiner, and N. C. Paek. 2014. "Delayed Degradation of Chlorophylls and Photosynthetic Proteins in *Arabidopsis* Autophagy Mutants During Stress-Induced Leaf Yellowing." *Journal of Experimental Botany* 65: 3915–3925.

Singh, A., B. Ganapathysubramanian, A. K. Singh, and S. Sarkar. 2016. "Machine Learning for High-Throughput Stress Phenotyping in Plants." *Trends in Plant Science* 21: 110–124.

Starý, K., Z. Jelínek, J. Kumhálova, J. Chyba, and K. Balážová. 2020. "Comparing RGB-Based Vegetation Indices From UAV Imageries to Estimate Hops Canopy Area. Agronomy." *Research* 18: 2592–2601.

Statista. 2023. Statista. https://www.statista.com/statistics/218984/number-of-global-mobile-users-since-2010/.

Stokes, M., M. Anderson, S. Chandrasekar, and R. Motta 1996. A Standard Default Color Space for the Internet—sRGB. https://www.w3.org/Graphics/Color/sRGB.html. Accessed July 2023.

Tao, H., S. Xu, Y. Tian, et al. 2022. "Proximal and Remote Sensing in Plant Phenomics: 20 Years of Progress, Challenges, and Perspectives." *Plant Communications* 3: 100344.

Trussell, J., E. Saber, and M. J. Vrhel. 2005. "Color Image Processing: Basics and Special Issue Overview." *IEEE Signal Processing Magazine* 22: 23–33.

Tsaftaris, S. A., M. Minervini, and H. Scharr. 2016. "Machine Learning for Plant Phenotyping Needs Image Processing." *Trends in Plant Science* 21: 989–991.

Valluvan, A. B., R. Raj, R. Pingale, and A. Jagarlapudi. 2023. "Canopy Height Estimation Using Drone-Based RGB Images." *Smart Agricultural Technology* 4: 100145.

Webster, M. A. 2009. "Human colour perception and its adaptation." *Network: Computation in Neural Systems* 7: 587–634. https://doi.org/10.1088/0954-898X_7_4_002.

Wellburn, A. R. 1994. "The Spectral Determination of Chlorophylls a and b, as well as Total Carotenoids, Using Various Solvents With Spectrophotometers of Different Resolution." *Journal of Plant Physiology* 144: 307–313.

Widlowski, J. L., M. M. Verstraete, B. Pinty, and N. Gobron. 2000. "Advanced Vegetation Indices Optimized for Up-Coming Sensors: Design, Performance, and Applications." *IEEE Transactions on Geoscience and Remote Sensing* 38: 2489–2505.

Wijerathna-Yapa, A., S. Signorelli, R. Fenske, et al. 2021. "Autophagy Mutants Show Delayed Chloroplast Development During De-Etiolation in Carbon Limiting Conditions." *Plant Journal* 108: 459–477.

Woebbecke, D. M., G. E. Meyer, K. Von Bargen, and D. A. Mortensen. 1995. "Color Indices for Weed Identification Under Various Soil, Residue, and Lighting Conditions." *Transactions of the American Society of Agricultural Engineers* 38: 259–269.

Wu, Q., Z. Chen, W. Sun, T. Deng, and M. Chen. 2016. "De Novo Sequencing of the Leaf Transcriptome Reveals Complex Light-Responsive Regulatory Networks in *Camellia sinensis* cv. Baijiguan." *Frontiers in Plant Science* 7: 1–15.

Yuan, Y., L. Chen, M. Li, N. Wu, L. Wan, and S. Wang. 2017. "Diagnosis of Nitrogen Nutrition of Rice Based on Image Processing of Visible

Light." *Proceedings—2016 IEEE International Conference on Functional-Structural Plant Growth Modeling, Simulation, Visualization and Applications, FSPMA* 2016: 228–232.

Zavafer, A., H. Bates, C. Mancilla, and P. J. Ralph. 2023. "Phenomics: Conceptualization and Importance for Plant Physiology." *Trends in Plant Science* 28: 1004–1013. https://doi.org/10.1016/J.TPLANTS.2023.03.023.

Supporting Information

Additional supporting information can be found online in the Supporting Information section.
Supplemental figure 1: Analysis of greenness in a 24-colour card for de optimization of our GI formula. **Supplemental Figure 2:** Pearson correlation between GI and total chlorophyll content. **Supplemental Figure 3:** Analysis of the scores obtained by multiple methods based on RGB values in plant images. **Supplemental Figure 4:** Green Index of arabidopsis leaves exposed to 150 mM NaCl. Supplemental Video.